Molecular Docking, Dynamics Simulation, and Scanning Electron Microscopy (SEM) Examination of Clinically Isolated *Mycobacterium tuberculosis* by Ursolic Acid: A Pentacyclic Triterpenes

Dian Ayu Eka Pitaloka[1,*], Sophi Damayanti[2], Aluicia Anita Artarini[3], and Elin Yulinah Sukandar[4]

[1]*Department Pharmacology-Clinical Pharmacy, School of Pharmacy, Institut Teknologi Bandung, Jl. Ganesa no. 10, Bandung 40132, West Java, Indonesia*

[2]*Department of Pharmacochemistry, School of Pharmacy, Institut Teknologi Bandung, Jl. Ganesa no. 10, Bandung 40132, West Java, Indonesia*

[3]*Department of Pharmaceutical Biotechnology, School of Pharmacy, Institut Teknologi Bandung, Jl. Ganesa no. 10, Bandung 40132, West Java, Indonesia*

[4]*Department of Pharmacology and Clinical Pharmacy, School of Pharmacy, Institut Teknologi Bandung, Jl. Ganesa no. 10, Bandung 40132, West Java, Indonesia*

* ***Corresponding author:***

email: dianayuekapitaloka@gmail.com

Received: March 6, 2018
Accepted: August 3, 2018

DOI: 10.22146/ijc.33731

Abstract: *The purpose of this study was to analyze the inhibitory action of ursolic acid (UA) as an antitubercular agent by computational docking studies and molecular dynamics simulations. The effect of UA on the cell wall of Mycobacterium tuberculosis (MTB) was evaluated by using Scanning Electron Microscopy (SEM). UA was used as a ligand for molecular interaction and investigate its binding activities to a group of proteins involved in the growth of MTB and the biosynthesis of the cell wall. Computational docking analysis was performed by using autodock 4.2.6 based on scoring functions. UA binding was confirmed by 30 ns molecular dynamics simulation using gromacs 5.1.1. H37Rv sensitive strain and isoniazid-resistant strain were used in the SEM study. UA showed to have the optimum binding affinity to inhA (Two-trans-enoyl-ACP reductase enzyme involved in elongation of fatty acid) with the binding energy of -9.2 kcal/mol. The dynamic simulation showed that the UA-inhA complex relatively stable and found to establish hydrogen bond with Thr196 and Ile194. SEM analysis confirms that UA treatment in both sensitive strain and resistant strain affected the morphology cell wall of MTB. This result indicated that UA could be one of the potential ligands for the development of new antituberculosis drugs.*

Keywords: *antituberculosis; ursolic acid; docking molecular; molecular dynamics simulation; Scanning Electron Microscopy (SEM)*

■ INTRODUCTION

Tuberculosis (TB) is an infectious disease that includes the ten most common cause of death in the world [1]. WHO [2] has reported that more than 30% of the world's population is infected with *Mycobacterium tuberculosis* (MTB) and 10% of that population become active patients during their lifetime. The control of this disease is getting difficult nowadays because of the Multidrug-Resistant (MDR) TB strains phenomena and its association with Human Immunodeficiency Virus (HIV). In 2014, 4,800,000 people developed MDR-TB in the world and 1.9% of TB cases with MDR-TB in Indonesia [3]. Based on that fact, new antituberculosis (anti-TB) agents that are effective in TB treatment need to be discovered.

Ursolic acid (3β-hydroxyl-12-en-28-oic acid) (UA) belongs to pentacyclic triterpenoid that widely found in numerous plants and several herbal medicines [4]. This compound is well-known to have various biological

activities including anti-inflammatory [5], anticancer [6], antioxidant [7-9] and antibacterial [6]. The study of the antibacterial properties of pentacyclic triterpenoids [10-11] and the activity of these compounds has been shown can enhance bacterial susceptibility to other compounds, including antibiotics [12]. *In vitro* study of UA found that it has activity as anti-TB with Minimum Inhibitory Concentration (MIC) in sensitive and resistant strains of MTB. UA has also displayed a synergistic interaction when combined with isoniazid (INH), rifampicin, ethambutol, and streptomycin [13]. The *in vivo* study was also found that UA showed a significant reduction of activity in rats induced by MTB H37Rv sensitive strain and MDR strains [14]. However, the *in silico* study of UA to proteins in MTB and the mechanism of action of this compound are still unclear and limited.

There are various proteins involved in the biogenesis of the cell wall and physiological functions of MTB have become targets for the development of anti-TB drugs. Two-trans-enoyl-ACP reductase (InhA) and β-ketoacyl-ACP reductase (MabA) are inhibited by isoniazid (INH) which is known as front-line anti-TB drugs [15-16]. These proteins are responsible for the production of long chain fatty acid derivatives that are key precursors to mycolic acids and belong to the type-II fatty acid elongation system (FAS-II) [15,17]. They display the same specificity for long-chain substrates and are similarly inhibited by the front-line anti-TB drug INH. Another target is the protein pantothenate kinase (PanK, type I) from pantothenic acid which is known to be essential for the growth of MTB and involved as a cofactor in the biosynthesis of Coenzyme A (CoA) [18]. PKS18 and PKS11 proteins are found in the cell envelope of MTB and important in the biosynthesis of long-chain α pyrones to construct the mycolic acid and multi methyl-branched fatty acid. RNA polymerase β subunit (rpoB) is a protein encoded by rpoB gene that important in the biosynthesis of a protein essential of MTB. Rifampicin is an anti-TB drug which is known to inhibit this protein [19-20].

The aim of this study was to test the efficiency of UA against some receptors in MTB using molecular docking studies. For further study, the best interaction occurred between UA as ligand and proteins as receptor were evaluated using molecular dynamics simulations. The effect of UA in cell walls of MTB was also evaluated by Scanning Electron Microscopy (SEM).

■ EXPERIMENTAL SECTION

Macromolecule Preparation

The crystal structure of MTB InhA (1BVR), mabA (1UZN), panK type 1 (3AF3), PKS 18 (1TED), rpoB (5HUB), and Gyrase B (4BAE) were obtained from the Protein Data Bank (RCSB PDB, https://www.rcsb.org/). The PDB file was prepared using software discovery studio. Discovery Studio Visualizer (DSV) v16.1.0.15350, was used to remove all water molecules and heteroatoms. The ligand binding domains of MTB InhA, mabA, panK type 1, PKS 18, rpoB, and gyrase B were also predicted using DSV v16.1.0.153500 software.

Ligand Preparation

UA as a ligand structure was built with MarvinSketch and the geometry structure was optimized by using Gaussian09 on the Austin Model 1 (AM1) semi-empirical method. The calculation used the Gasteiger charge and added partial charges to the ligand atoms prior to docking [21]. After minimization of the energy conformation, the structure with the lowest energy was selected and prepared for docking study.

Molecular Docking Analysis

The molecular docking analysis between UA in the active sites of MTB proteins was performed by using software autodock 4.2.6.Autodock Tools (ADT) was used to set the Grid box parameters [22-23]. All the six targets and ligand were prepared by addition of hydrogens and Gasteiger charges. The docking process was also used the Lamarckian genetic algorithm to get the best conformation between ligand and receptor with the population size of 100 individuals.

Molecular Dynamics Simulation Protocol

Minimization of potential energy and MD simulations were run using GROMACS 5.1.1. AMBER99SB-ILDN was used as a force field in its simulations and AnteChamber Python Parser interface (ACPYPE) was used to parameterize the topologies,

atomic types, and charges [24]. The protein complexes were solvated by cubic explicit water molecules solvent. The parameter conditions such as pressure and the temperature were maintained constant during the simulation. Sodium and chlorine ion was added to the system as simulation setup neutralizer. Energy minimized structures of the protein complex was used as a starting point for MD simulations. Production runs of 30 ns with an integration time step of 0.2 ps were performed at a constant temperature and pressure using the leapfrog algorithm. LINCS algorithm was used to constrain all bonds during the equilibration while the particle-mesh Ewald algorithm approximated long-range ionic interactions. Trajectory snapshots were stored at every 0.2 ps during the simulation period, and 3D coordinate files harvested after every 2 ns for post-dynamic analysis.

Analysis of Trajectory Files

Root-Mean-Square Deviation (RMSD) and Root-Mean-Square Fluctuation (RMSF) were analyzed through the use of g_rmsd and g_rmsf respectively. It was determined on the basis of donor-hydrogen acceptor angle greater than 90 nm and donor-acceptor distance lesser than 3.9 nm [25].

Microorganism

Clinically isolated H37Rv sensitive strain and INH resistant strain of MTB was used as microorganisms in this study. All bacterias were provided from the Laboratory of Health Development, West Java Province. Bacterial strains were maintained by subculture on Lowenstein Jensen (LJ) media for 3 weeks at 37 °C for their favorable growth.

Reagents and Antibiotics

Antibiotics INH and UA were purchased from Sigma Aldrich for the study and drug control. INH was prepared in deionized water. Dimethyl sulfoxide (DMSO) (Merck) was used as a solvent for UA with the concentration of 0.5% v/v [26].

Determination of Minimum Inhibitory Concentration (MIC)

The antimycobacterial activity of UA against two different strains of MTB was tested by susceptibility test using proportion methods in LJ media. Mc Farland no.1 turbidity standard was used as the comparison to get the inoculum 3×106 cfu/mL and 100 µL bacteria suspension containing approximately 3×105 cfu/mL were spotted onto LJ media in Mc Cartney tubes. Cultivation was done at 37 °C for 8 weeks and MICs were read as minimum concentrations of drugs completely inhibiting visible growth of the organisms.

Preparation of Cells for SEM

The preparation of cells for SEM study was done as described by Jyoti et al. [27]. MTB cells in their early log phase were washed by PBS and harvested by centrifugation. Approximately, an equal amount of cells were suspended in 7H9-S media and treated with UA and INH at their 10×MIC concentration for 24 h in 37 °C. After that, MTB Cells were centrifugated again at 3000 RCF for 10 min and washed with 0.1 M phosphate buffer pH 7.3. Glutaraldehyde 2.5% was used to fixed the cells for 24 h and washed again with 0.1 M PB. Continuously, osmium tetraoxide 2% in 01 M sodium cacodylate buffer was used in the post-fixation and washed again with PB as described earlier. Cells were then dehydrated in a series of ethanol gradient (50, 60, 70, 90, and 100% ethanol). After the preparation of the samples, bacteria surface was examined using Scanning Electron Microscopy SUE3500 (JEOL JMS-840 Japan) with the accelerating voltage of 5 kV. Microphotographs were taken at magnifications ranging from 500x to 10,000x.

■ RESULTS AND DISCUSSION

Ursolic acid (3β-hydroxyl-12-en-28-oic acid) is a pentacyclic triterpene in the form of free acid or aglycones for saponin triterpenes (Fig. 1) [28] in certain medicinal herbs and fruits [7]. It reported having a wide range of activities including anti mycobacteria and can inhibit the growth of MTB in both sensitive and resistant strains. It also is shown that UA has a synergistic effect when it combined with INH, rifampicin, ethambutol, or pyrazinamide [13]. In this research, UA acts as a ligand and docked on the site of drug action of the selected receptor of MTB which is responsible for the pharmaceutical effect.

Molecular Docking of Ursolic Acid

The present study helps us to understand the interaction between the ligand (UA) and proteins (receptors) and also explore their binding mode. Proteins as receptor were derived from PDB and used as a target for docking simulation. Ligand UA was prepared for the docking procedure using MarvinSkech and optimized using the semi-empirical method with AM1 as a basis set.

The docking study was performed using Autodock 4.2.6 and grid box parameters (Table 1) were set by using Autodock Tools (ADT) to re-docking between proteins and their nature ligand. The aim of these docking was to validate the software before UA was docking to the protein target. Root Mean Square Deviation (RMSD) was used as a validation parameter. Ideally, the quality of reproduction of binding pose by a computational method is good when RMSD value less than 2.0 Angstrom [29]. The grid box parameters selected for target proteins and their binding site were mentioned in Table 1. All the grid box parameters for these proteins have RMSD less than 2.0 Angstrom (Å).

Thr196 residue in the binding loop between NAD as native ligand and inhA has been found as a critical amino acid that helps to fix the NAD on to its active site. Moreover, the hydroxyl group of Ile194 residue in inhA (PDB ID:1BVR) is responsible for hydrogen bonding between inhA and NAD. In addition, the Tyr158 residue also plays a crucial role in the interaction and mutation in this residue to Ala94 causes MTB to become resistant to INH [30].

There are two amino acids which are associated with mabA enzymes, such as Tyr153 and Gly90. The Tyr153 residue has a central role in the acid-base catalysis performed by this enzyme [30] and Gly90 residue has been shown to be involved in the complexation of mabA with its natural ligand. It has been shown that mutation of Gle139 into Ala139 causes complete mabA inactivation by freezing the catalytic triad into a closed form [31].

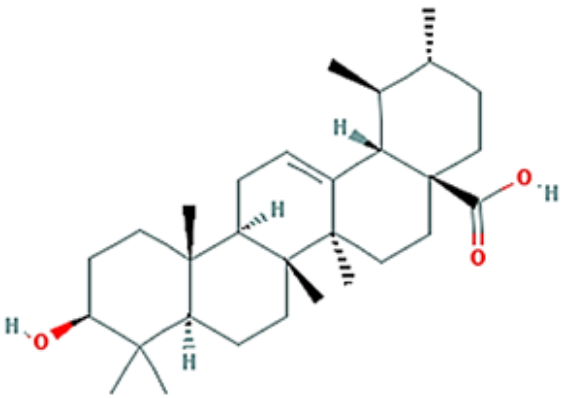

Fig 1. Chemical structure of UA (CID: 64945)

Table 1. Grid box parameter selected and binding site residues for the target proteins

Protein name	Center grid box (points)	Size (points)	Spacing (A)	Binding site
inhA (1BVR)	19.88x8.874x14.397	60x40x40	0.375	Pro193, Met199, Tyr158, Met161, Met147, ile21, Ser20, Ser94, ile194, ile95, Phe41, ile122, Val65, Phe149, Thr196
mabA (1UZN)	5.741x19.526x15.632	20x36x30	0.375	Ile27, Arg25, Gly22, Asn88, Arg47, Gly90, Ala89, Ala11, Val62, Ser140, Tyr153, Lys157
panK (3AF3)	-44.285x36.173x-4.171	20x18x20	0.375	Met242, Phe254, Tyr235, Phe247, Arg238, Gly97, Ala100, Val101, Ser104
Pks 18 (1TED)	6.644x15.142x4.950	40x40x40	0.375	Ser43, Cys275, Leu348, Leu266, Thr274, Cys205, ile273, Ala209, Asn208, Ala52, Val56, Arg81, Tyr73, Phe211, His221, Val47, Phe224
RpoB (5UHB)	6.387x5.621x0.208	48x58x48	0.375	Thr585, Ala586, Ala584, Thr829, Pro611, Leu612, Lys832, Pro834, Gly839, Gln861, Pro962, Val970, Thr968

PanK is a cofactor in the biosynthesis of Coenzyme (CoA) and responsible for the growth of MTB. The complex of panK protein with its native ligand found that amino acids Ala100 to Ser104 are known to be part of the PanK P-loop and responsible for the holding of ATP during catalysis [18,32]. Other amino acids (Arg238) acts as a connector between the phosphorylated pantothenate and ATP, thereby aiding catalysis [33].

A study conducted by Sankaranarayanan et al. [34] suggested that PKS 18 has specificity for aliphatic long-chain acyl CoA substrate and structural analysis suggested that amino acids Thr144, Cys205, and Ala209 have a crucial role in determining the cavity volume or binding site of the protein complex. In addition, the docking study conducted by Andrade et al. [35] showed the binding efficiency of rifampicin to the rpoB receptor was increased by the presence of a hydroxyl group at the para carbon position of the benzene ring is an auxophoric group.

The predicted binding free energies observed for UA with six different proteins which involved in growth and survival of MTB shown that UA has the highest affinity to inhA which belongs to type-II fatty acid elongation system (FAS II) in the cell wall, with the score was -9.30 kcal/mol (Table 2). UA was found to establish hydrogen bond with Thr196 and Ile194 (Fig. 2) and interacted with Tyr158 which previously said that plays a crucial role in the interaction of ligand and protein in the binding site.

Molecular Dynamic Simulation of Ursolic Acid

The molecular dynamics simulations were done to validate the *in silico* stability of UA-inhA complex and to find any correlation between them using in silico parameters such as the time of the dynamic process (in nanoseconds), the stability of the complex with Root Mean Square Deviation (RMSD) parameter in Angstrom, and the fluctuation residues in molecule with Root Mean Square Fluctuation parameter of atom. Fig. 3 shown that RMSD for the UA-inhA complex was less than 2.0 Å which indicated the stability of the complex during simulation. It also can be concluded that after 30 ns dynamic simulations, the endpoint was a stable complex where the position and the interactions of the ligand were not changed at all.

Beside the RMSD, the flexibility of protein was assessed using RMSF to indicate flexible regions in the

Table 2. Docking scores (predicted binding energies) between UA and the target protein

Protein name	Predicted binding energy of UA (kcal/mol)
inhA (1BVR)	-9.3
RpoB (5UHB)	-8.8
MabA (1UZN)	-6.6
Gyrase B (4BAE)	-4.5
PanK (3AF3)	1.8
Pks18 (1TED)	51.4

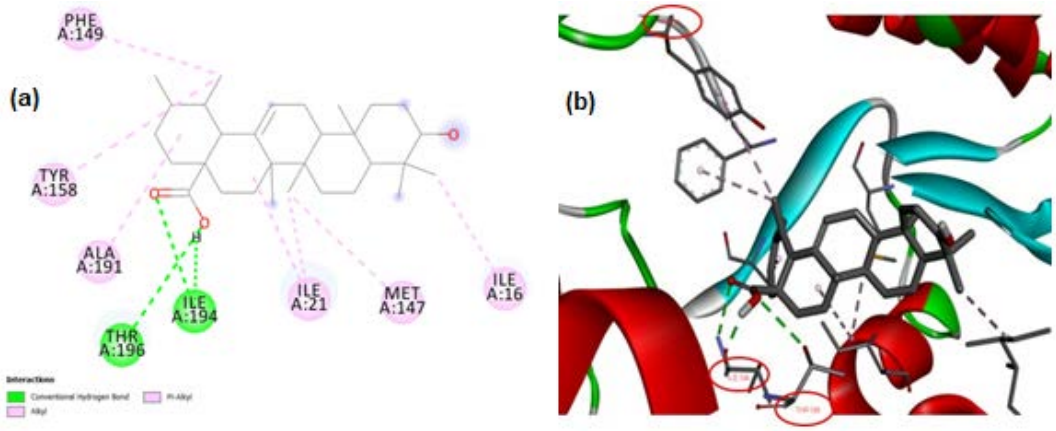

Fig 2. Molecular interactions between UA and inhA performed by Discovery Studio in 2D (a) and 3D (b)

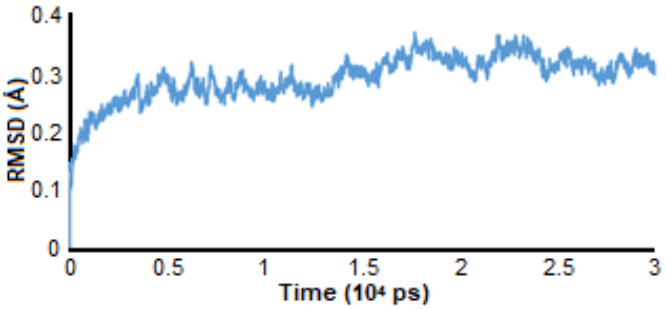

Fig 3. Root Mean Square Deviation (RMSD) of UA-inhA complex during 30 ns dynamics simulation

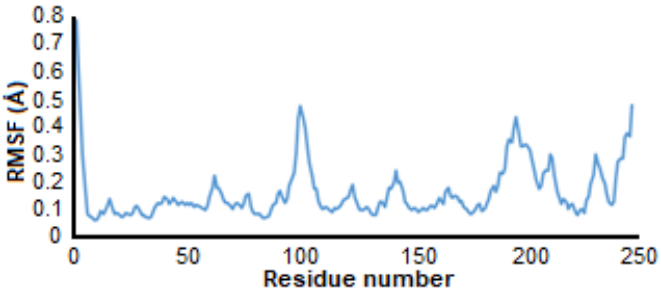

Fig 4. Root Mean Square Fluctuation (RMSF) of all residues in the inhA molecule during dynamics simulation

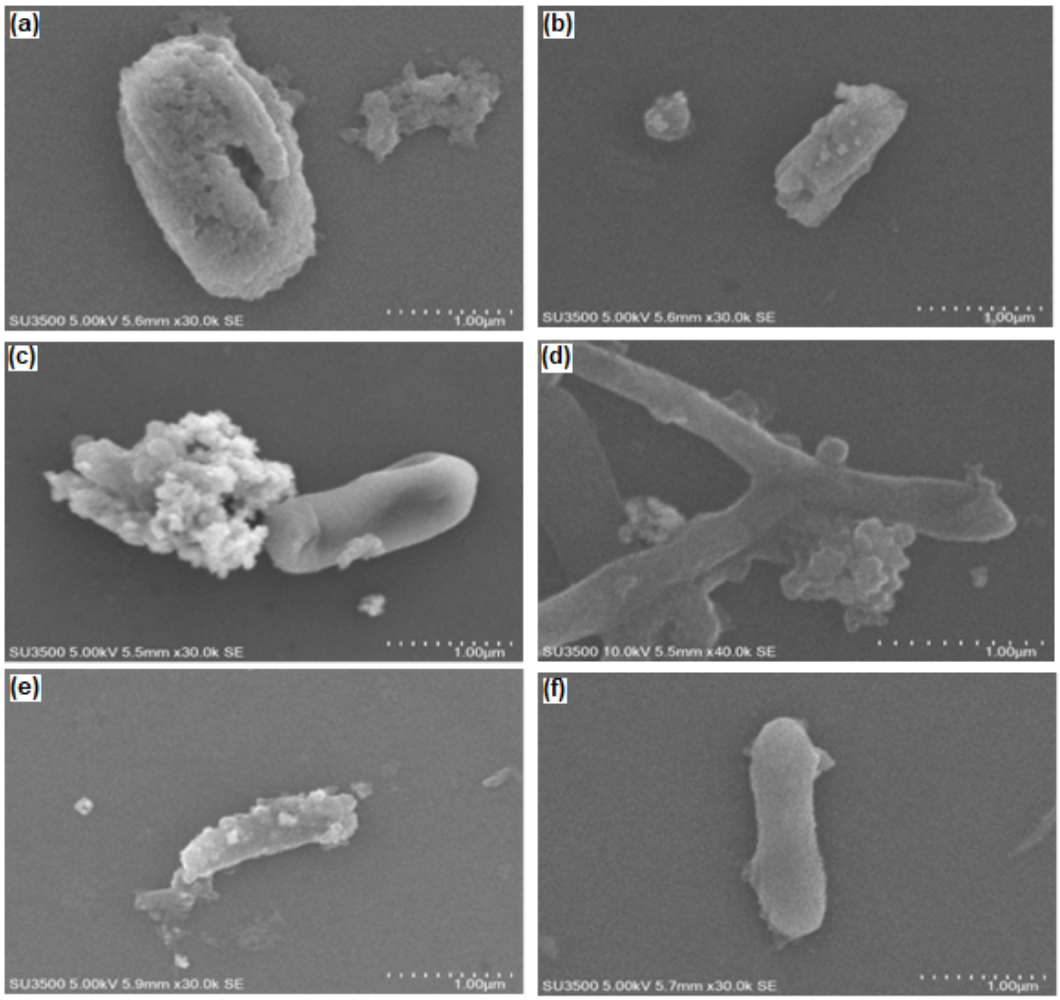

Fig 5. Scanning electron microscopy of H37Rv treated with UA (a), INH resistant treated with UA (b), H37Rv treated with INH (c), INH resistant treated with INH (d), non-treated INH resistant (e), non-treated H37Rv (f)

protein. It also evaluated the properties of rigid hinge residues and flexible hinge residues based on conformational properties. Based on Fig. 4, most of the protein residues in inhA had RMSF lower than 2.0 Å. It indicated that the UA binding as a ligand did not induce conformation change of inhA protein as a receptor target. The figure was also showed that threonine (residue position in 100 and 196) in random coil area has

a higher flexibility than other residues. It needs great attention especially in Thr196 because this residue is also responsible for the binding pocket of the protein and would affect the interaction and affinity of UA in the protein.

Scanning Electron Microscopy (SEM)

The aim of SEM analysis is to observe the cell structure of MTB. Micrographs images of MTB by SEM showed how UA and INH as drug control affected the morphology of the cell wall of MTB. Based on Fig. 5, the SEM micrographs of MTB sensitive H37Rv strain displayed distinguished signs of cell wall damage, including, deep craters, burst cells, and lysis. Most of the walls were actually missing and broken led to distorted shape. Outer membrane thickening indicated severe damage in MTB sensitive H37Rv. Otherwise, it seems UA did not effect of INH resistant strain of MTB because there were no signs of cell wall destruction as well as MTB sensitive H37Rv strains (Fig. 5). The normal appearing cocci of MTB could be found in the control in comparison to the treated MTB.

The previous study conducted by Jyoti et al. [28] using Transmission Electron Microscopy (TEM) showed that UA severely affected the cell wall peptidoglycan of H37Ra sensitive strain of MTB. The entire PG layer leaves the cell body caused by osmotic imbalance. The condensation of nucleic acid and protein materials was also found in the inner cytoplasmic of the cell because of UA efflux in the cytoplasm.

Based on these study, it can be concluded that the mechanism of action of UA against MTB may probably in the cell wall of MTB with specifically inhibit the inhA enzyme to elongate the biosynthesis of fatty acid as the precursor of mycolic acid.

■ CONCLUSION

We showed that UA effectively inhibited MTB *invitro*. Our study suggested that UA interferes biosynthesis of mycolic acid in the cell wall of MTB. It was also indicated by the computational approach and found that UA has the highest affinity for inhA enzyme which is responsible for the elongation of fatty acid (the precursor of mycolic acid) in FAS II System. UA was found to establish hydrogen bond with Thr196, Ile194 and interacted with Ser94 which previously said that plays a crucial role in the interaction of native ligand and enzyme in the binding site. For further study, we will continue the *in vitro* and *in vivo* study specifically in the FAS II system. Moreover, we will try to study the influence of UA in the host of the immune system.

■ ACKNOWLEDGMENTS

This research was supported by Directorate General of Resources for Science Technology and Higher Education of the Republic of Indonesia.

■ REFERENCES

[1] Ducati, R.G., Ruffino-Netto, A., Basso, L.A., and Santos, D.S., 2006, The resumption of consumption – A review on tuberculosis, *Mem. Inst. Oswaldo Cruz*, 101 (1), 697–714.

[2] Jassal, M.S., and Bishai, W.R., 2015, The epidemiology and challenges to the elimination of global tuberculosis, *Clin. Infect. Dis.*, 50 (Suppl. 3), 156–164.

[3] World Health Organization, *Tuberculosis*, http://www.who.int/, accessed on January 31, 2018.

[4] Kim, K.A., Lee, J.S., Park, H.J., Kim, C.J., Shim, I.S., Kim, N.J., Han, S.M., and Lim, S., 2004, Inhibition of cytochrome P450 activities by oleanolic acid and ursolic acid in human liver microsomes, *Life Sci.*, 74 (22), 2769–2779.

[5] Ku, C.M., and Lin, J.Y., 2013, Anti-inflammatory effects of 27 selected terpenoid compounds tested through modulating Th1/Th2 cytokine secretion profiles using murine primary splenocytes, *Food Chem.*, 141 (2), 1104–1113.

[6] Shanmugam, M.K., Dai, X., Kumar, A.P., Tan, B.K.H., Sethi, G., and Bishayee, A., 2013, Ursolic acid in cancer prevention and treatment: Molecular targets, pharmacokinetics and clinical studies, *Biochem. Pharmacol.*, 85 (11), 1579–1587.

[7] Liobikas, J., Majiene, D., Trumbeckaite, S, Kursvietiene, L., Masteikova, R., Kopustinskiene, D.M., Savickas, A., and Bernatoniene, J., 2011, Uncoupling and antioxidant effects of ursolic acid

in isolated rat heart mitochondria, *J. Nat. Prod.*, 74 (7), 1640–1644.

[8] Ali, M.S., Ibrahim, S.A., Jalil, S., and Choudhary, M.I., 2007, Ursolic acid: A potent inhibitor of superoxides produced in the cellular system, *Phytother. Res.*, 21 (6), 558–561.

[9] D'Abrosca, B., Fiorentino, A., Monaco, P., and Pacifico, S., 2005, Radical-scavenging activities of new hydroxylated ursane triterpenes from cv. Annurca apples, *Chem. Biodivers.*, 2 (7), 953–958.

[10] Mallavadhani, U.V., Mahapatra, A., Jamil, K., and Reddy, P.S., 2004, Antimicrobial activity of some pentacyclic triterpenes and their synthesized 3-*O*-lipophilic chains, *Biol. Pharm. Bull.*, 27 (10), 1576–1579.

[11] Silva, M.L., David, J.P., Silva, L.C.R.C., Santos, R.A.F., David, J.M., Lima, L.S., Reis, P.S., and Fontana, R., 2012, Bioactive oleanane, lupane and ursane triterpene acid derivatives, *Molecules*, 17 (10), 12197–12205.

[12] Kurek, A., Nadkowska, P., Pliszka, S., and Wolska, K.I., 2012, Modulation of antibiotic resistance in bacterial pathogens by oleanolic acid and ursolic acid, *Phytomedicine*, 19 (6), 515–519.

[13] Pitaloka, D.A.E., and Sukandar, E.Y., 2017, *In vitro* study of ursolic acid combination first-line antituberculosis drugs against drug-sensitive and drug-resistant strains of *Mycobacterium tuberculosis*, *Asian J. Pharm. Clin. Res.*, 10 (4), 216–218.

[14] Martins, D., Carrion, L.L., Ramos, D.F., Salomé, K.S., da Silva, P.E.A., Andersson, B., Cleverson Agner Ramos, C.A., and Cecilia Veronica Nunez, C.V., 2014, Anti-tuberculosis activity of oleanolic and ursolic acid isolated from the dichloromethane extract of leaves from *Duroia macrophylla*, *BMC Proc.*, 8 (Suppl. 4), P3.

[15] Marrakchi, H., Lanéelle, G., and Quémard, A., 2010, InhA, a target of the antituberculous drug isoniazid is involved in a mycobacterial fatty acid elongation system, FAS-II, *Microbiology*, 146 (2), 289–296.

[16] Ducasse-Cabanot, S., Cohen-Gonsaud, M., Marrakchi, H., Nguyen, M., Zerbib, D., Bernadou, J., Daffé, M., Labesse, G., and Quémard, A., 2004, *In vitro* inhibition of the *Mycobacterium tuberculosis* β-ketoacyl-acyl carrier protein reductase MabA by isoniazid, *Antimicrob. Agents Chemother.*, 48 (1), 242–249.

[17] Takayama, K., Wang, C., and Besra, G.S., 2005, Pathway to synthesis and processing of mycolic acids in *Mycobacterium tuberculosis*, *Clin. Microbiol. Rev.*, 18 (1), 81–101.

[18] Björkelid, C., Bergfors, T., Raichurkar, A.K., Mukherjee, K., Malolanarasimhan, K., Bandodkar, B., and Jones, T.A., 2013, Structural and biochemical characterization of compounds inhibiting *Mycobacterium tuberculosis* pantothenate kinase, *J. Biol. Chem.*, 208 (25), 18260–18270.

[19] Ramaswamy, S., and Musser, J.M., 1998, Molecular genetic basis of antimicrobial agent resistance in *Mycobacterium tuberculosis*: 1998 update, *Tuber. Lung Dis.*, 79 (1), 3–29.

[20] Campbell, E.A., Korzheva, N., Mustaev, A., Murakami, K., Nair, S., Goldfarb, A., and Darst, S.A., 2011, Structural mechanism for Rifampicin inhibition of bacterial RNA polymerase, *Cell*, 104 (6), 901–912.

[21] Gasteiger, J., and Marsili, M., 1980, Iterative partial equalization of orbital electronegativity-a rapid access to atomic charges, *Tetrahedron*, 36 (22), 3219–3228.

[22] Goodsell, D.S., Morris, G.M., and Olson, A.J., 1996, Automated docking of flexible ligands: applications of autodock, *J. Mol. Recognit.*, 9 (1), 1–5.

[23] Morris, G.M., Goodsell, D.S., Halliday, R.S., Huey, R., Hart, W.E., Belew, R.K., and Olson, A.J., 1998, Automated docking using a Lamarckian genetic algorithm and an empirical binding free energy function, *J. Comput. Chem.*, 19 (14), 1639–1662.

[24] Caims, D., Michalitsi, E., Jenkins, T.C., and Mackay, S.P., 2002, Molecular modelling and cytotoxicity of substituted anthraquinones as inhibitors of human telomerase, *Bioorg. Med. Chem.*, 10 (3), 803–807.

[25] Humphrey, W., Dalke, A., and Schulten, K., 1996, VMD: Visual molecular dynamics, *J. Mol. Graphics*, 14 (1), 33–38.

[26] De Logu, A., Onnis, V., Saddi, B., Congiu, C., Schivo, M.L., and Cocco, M.T., 2002, Activity of a new class of isonicotinoylhydrazones used alone and in combination with isoniazid, rifampicin, ethambutol, para-aminosalicylic acid and clofazimine against *Mycobacterium tuberculosis*, *J. Antimicrob. Chemother.*, 49 (2), 275–282.

[27] Jyoti, M.A., Zerin, T., Kim, T.H., Hwang, T.S., Jang, W.S., Nam, K.W., and Song, H.Y., 2015, *In vitro* effect of ursolic acid on the inhibition of *Mycobacterium tuberculosis* and its cell wall mycolic acid, *Pulm. Pharmacol. Ther.*, 33, 17–24.

[28] Zhang Y., and Yew, W.W., 2015, Mechanism of drug resistance in *Mycobacterium tuberculosis*: Update 2015, *Int. J. Tuberc. Lung Dis.*, 19 (11), 1276–1289

[29] Shoichet, B.K., McGovern, S.L., Wei, B., and Irwin, J.J., 2002, Lead discovery using molecular docking, *Curr. Opin. Chem. Biol.*, 6 (4), 436–446.

[30] Rozwarski, D.A., Vilchèze, C., Sugantino, M., Bittman, R., and Sacchettini, J.C., 1999, Crystal structure of the Mycobacterium tuberculosis enoyl-ACP reductase, InhA, in complex with NAD^+ and a C16 fatty acyl substrate, *J. Biol. Chem.*, 274 (22), 15582–15589.

[31] Rosado, L.A., Caceres, R.A., de Azevedo Jr, W.F., Basso, L.A., and Santos, D.S., 2012, Role of serine140 in the mode of action of *Mycobacterium tuberculosis* β-ketoacyl-ACP reductase (MabA), *BMC Res. Note*, 5, 526.

[32] Cheek, S., Zhang, H., and Grishin, N.V., 2002, Sequence and structure classification of kinases, *J. Mol. Biol.*, 320 (4), 855–881.

[33] Chetnani, B., Kumar, P., Surolia, A., and Vijayan, M., 2010, *M. tuberculosis* pantothenate kinase: Dual substrate specificity and unusual changes in ligand locations, *J. Mol. Biol.*, 400 (2), 171–185.

[34] Sankaranarayanan, R., Saxena, P., Marathe, U.B., Gokhale, R.S., Shanmugam, V.M., and Rukmini, R., 2004, A novel tunnel in mycobacterial type III polypeptide synthase reveals the structural basis for generating diverse metabolites, *Nat. Struct. Mol. Biol.*, 11 (9), 894–900.

[35] Andrade, B., Souza, C., and Goes-Neto, A., 2013, Molecular docking between the RNA polymerase of the *Moniliophthora perniciosa* mitochondrial plasmid and rifampicin produces a highly stable complex, *Theor. Biol. Med. Modell.*, 10 (15), 10–15.